ISSN:2790-1688 Volume-5-(2023)

Comparative Analysis of Finite Element Simulation and Experiment on the Polished Surface Quality of Hard Anodized Film of Aluminum Alloy

Zeliang Wang[1, a], Bing Tian[2, b], Qingguo Meng[1, c], and Jing Lu[1, d]

[1] Dalian Changfeng Industrial Corporation, Mechanical processing workshop, Dalian, Liaoning 116000

[2] Dalian Changfeng Industrial Corporation, Technology Center, Dalian, Liaoning 116000

[a] 66634970@qq.com, [b] 928195166@qq.com, [c] 873290770@qq.com, [d] 1183112766@qq.com

Abstract. According to the abrasive morphology and distribution of sandpaper surface, the finite element model of hard anodic oxide film polishing was established by using ABAQUS finite element software, and the hard anodic oxide film and aluminum alloy matrix were defined respectively. The effects of hard anodic oxide film polishing process, polishing surface quality and polishing parameters on the polishing force were simulated. The polishing surface quality and polishing force simulated by finite element model were verified by experiments. The results show that in the polishing process, the residual stress of polishing surface is mainly distributed in the range of 0.0034mm, and the chips produced by polishing are mainly broken and long strips with microscopic morphology, and polishing mainly depends on the front part of abrasive particles in the feeding direction of sandpaper. Under the action of abrasive particles of sandpaper, the results of finite element simulation and test show that there are certain grooves on the surface of oxide film. The finite element simulation of the normal polishing force of hard anodic oxide film is consistent with the polishing test results. During the process of polishing hard anodic oxide film, the normal polishing force increases as the polishing speed increases; the normal polishing force increases as the polishing removal amount increases; the polishing removal amount parameter has a greater degree of influence on the polishing force.

Keywords: hard anodic oxide film; polishing force; finite element; surface morphology.

1. Introduction

2D70 aluminum alloy, as an Al-Cu-Mg-Fe-Ni system aluminum alloy, has good plasticity and heat resistance properties and excellent comprehensive mechanical properties, and is widely used in aerospace, automobile industry and other fields [1], However, its low hardness and poor wear resistance limit its application range. The oxide film layer obtained by hard anodizing of aluminum alloys is thicker, has high hardness, good wear resistance, and is firmly bonded to the matrix. Therefore, aluminum alloy hard anodizing is widely used in the surface protection technology of aluminum alloy products [2-6]. Hard anodized films has high corrosion resistance in the atmosphere, high wear resistance, and a series of advantages such as strong bonding with the matrix metal. At present, there are few researches on the hard anodic oxide film polishing of aluminum alloy, Wenbo Pan et al. adopted cluster magnetorheological plane polishing technology to carry out polishing experiments on the anodized film of aluminum alloy, and discussed the influence of processing parameters such as machining clearance, workpiece rotation speed, disc rotation speed, yaw amplitude and processing time on its surface roughness and material removal rate [7]. Wielage found that proper pretreatment of aluminum alloy ENAW-6082 could change the growth rate and surface morphology of hard anodic oxide film [8]. Hongqiang Wan et al. used ANSYS Workbench software to analyze the changes of workpiece surface structure and stress under ultrasonic vibration conditions and ultrasonic composite abrasive vibration conditions, respectively [9].

There are few researches on hard anodizing film polishing of 2D70 aluminum alloy hard anodic oxide film. The finite element analysis was conducted for the polishing of 2D70 aluminum alloy hard anodic oxide film, and the results were compared with the experiments to analyze and study

the polishing process and polishing surface morphology, as well as the trend of polishing force under different polishing conditions, which is of guiding significance for the polishing of aluminum alloy hard anodic oxide layer.

2. The establishment of finite element model

2.1 The surface topography of sandpaper

Sandpaper is composed of a large number of irregularly shaped abrasive particles randomly combined on the substrate by electrostatic adsorption. Different from general tools, the abrasive particles on the surface of sandpaper are randomly distributed. The surface topography of sandpaper represents the distribution and shape of abrasive particles on the surface of the substrate, which directly affects the polishing force and surface polishing quality of the workpiece in the polishing process. And establishing a model to accurately describe the surface morphology of sandpaper is the key to realize the simulation of polishing process. In this paper, the study is conducted for the Microfinishing Film (15μm) sandpaper produced by 3M, and the local microscopic morphology of the surface of the sandpaper is observed and analyzed by JSM-IT800, a Japanese electronic scanning electron microscope with a maximum magnification of 2 million and a resolution of nanometer level, and the local abrasive surface morphology of the sandpaper is measured as shown in Fig. 1.

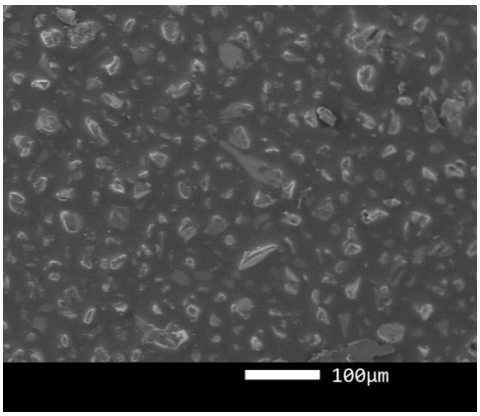

Fig. 1 The abrasive surface morphology of sandpaper

A large number of abrasive grains are randomly distributed on the surface of sandpaper, and the shape of abrasive grains is irregular polyhedron. In order to truly reflect the internal stress distribution of the oxide film during the polishing process of the hard anodic oxide film of aluminum alloy, a simulation model is established against the shape and distribution state of the abrasive grains on the surface of the sandpaper as shown in Fig. 1.

2.2 The establishment of finite element model

ABAQUS/Explicit uses the explicit integral of time to solve the dynamic finite element equation. In order to truly reflect the stress field distribution and polishing forces inside the workpiece during the polishing process, the models of hard anodic oxide film and aluminum alloy matrix are established respectively. The finite element model mesh of hard anodic oxide film adopts C3D8R eight-node linear hexahedral element, which is discretized into 450000 mesh elements with a element length of 0.002mm by free mesh method; the finite element model mesh of aluminum alloy substrate adopts C3D8R, namely eight-node linear hexahedral element, which is discretized into 221100 mesh element s with a element length of 0.003mm by free mesh method. 0.003mm.The hard anodic oxide film and aluminum alloy matrix are assembled together by binding constraints, which can make the contact surface of the hard anodic oxide film and aluminum alloy matrix have sufficient bonding strength. The sandpaper model refers to the abrasive surface morphology of sandpaper shown in Fig. 1, and adopts C3D4 four-node linear tetrahedral elements, which are

discretized into 176158 mesh element s with a element length of 0.004mm. The finite element model of sandpaper is shown in Fig. 2.

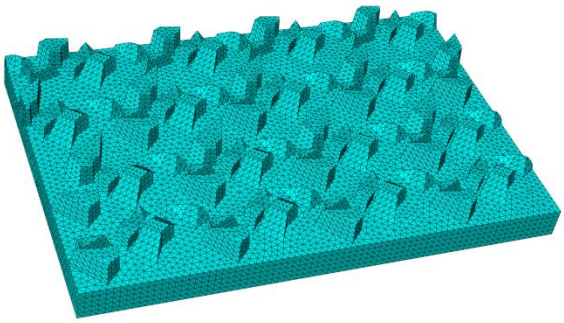

Fig. 2 The finite element model of sandpaper

In defining the contact pair of sandpaper and workpiece, the outer surface of sandpaper abrasive grain is defined as the main contact surface in the contact pair, and the nodal area of hard anodized film is defined as the slave contact surface. There is friction between abrasive and workpiece in the cutting process, and the friction is divided into normal friction and tangential friction in ABAQUS finite element software, with normal defined as frictionless hard contact and tangential defined as penalty friction, and the friction coefficient is generally taken as 0.3. The simplified 3D polishing finite element model is shown in Fig. 3. The total length of the workpiece is 0.3mm, the width is 0.2mm, and the height is 0.16mm, where the thickness of the hard anodized film is 0.06mm and the aluminum alloy substrate is 0.1mm.All the degrees of freedom at the bottom of the model are constrained under the initial conditions to ensure that no translation or rotation of the workpiece occurs during the polishing process. The abrasive grain is rigidly bound to the constraint, assuming that the abrasive grain stiffness is infinite, no deformation and wear phenomenon will occur during the cutting process, and the Y-axis direction is the feeding direction of the sandpaper. In the actual polishing process, the workpiece is generally polished by rotating with sandpaper, and considering the small size of the simulation model and the short calculation time, the motion of the sandpaper abrasive grain is approximated as a linear motion.

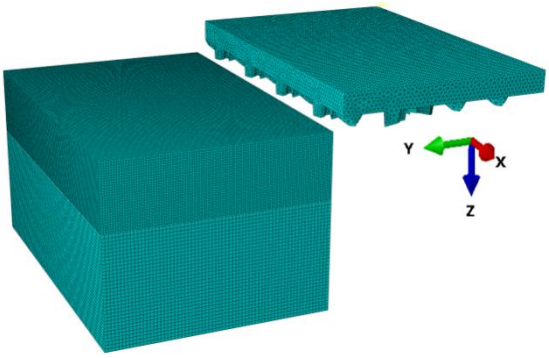

Fig. 3 The finite element analysis model of aluminum alloy hard anodized film polishing

2.3 Material properties and constitutive relations

Table 1. The material properties [10]

	Density ρ （kg/m3）	elasticity modulus E（GPa）	Poisson's ratio γ	coefficient of thermal expansion （10E-6）	Conductivity k（W/m•K）
2D70 aluminum alloy matrix	2700	7.00E+10	0.3	2.35E-5	162
hard anodic oxide film	3890	3.75E+11	0.22	8.4E-6	20

The base material properties of aluminum alloy hard oxide film and the base material of 2D70 aluminum alloy matrix are shown in Table 1, and Johnson-Cook parameters are shown in Table 2, where *A* is the yield strength, *B* is the strain hardening coefficient, *C* is the strain rate coefficient, *m* is temperature sensitivity coefficient and *n* is the strain hardening index.

Table 2. Johnson-Cook parameters of 2D70 aluminum alloy [11]

material	A	B	n	m	melting temperature	environment temperature
beryllium bronze	176.45Mpa	63.99Mpa	0.07	0	923K	293K

2.4 Simulation conditions

The single factor simulation analysis method was used to study the workpiece stress distribution and polishing force in the polishing process of aluminum alloy hard anodic oxide film under different polishing speed and polishing removal conditions, and the finite element simulation conditions are shown in Table 3.

Table 3. The finite element simulation conditions

parameter	value
polishing speed v（m/min）	31、40、50、56、62、70
polishing removal conditions（mm）	0.001、0.002、0.003、0.004

3. Polishing test

In order to verify the effectiveness of the finite element model, the polishing test of aluminum alloy hard oxide film was carried out on the CM6140A precision ordinary lathe, whose spindle could realize 24-stage speed regulation between 10r/min and 1400r/min, and the polishing experimental system is shown in Fig. 4(a).The polishing force measurement system is shown in Fig. 4(b), includes a handheld digital LCD meter MCK-HY instrument sensor and a JLBM tie rod diaphragm cassette type pulling pressure sensor, which can realize the measurement of polishing force. The surface micromorphology of polished hard oxide film of aluminum alloy was observed and analyzed by a Japanese electronic scanning electron microscope JSM-IT800.

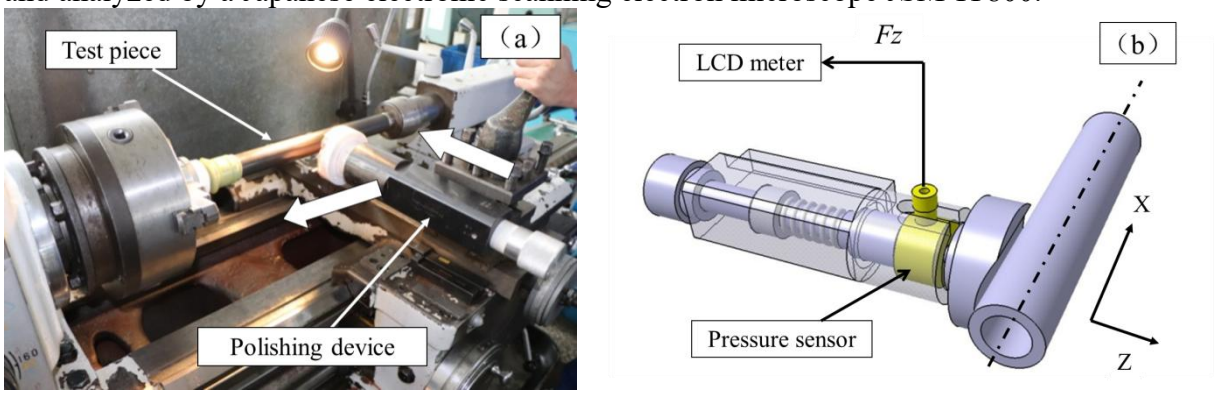

(a) the polishing experimental system (b) The polishing force measurement system

Fig. 4 The schematic diagram of the polishing experimental system and polishing force measurement system

The dimensions of the aluminum alloy hard oxide film polishing test pieces used in the experiment are: Φ 40mm × 350mm, the matrix is 2D70 aluminum alloy, the surface layer is the hard anodic oxide film, and the thickness is 60 ～ 70 μ m. The experiment is a single-factor experiment, and the experimental variables were respectively normal polishing force *Fz* and polishing speed v. The single-factor test parameters are shown in Table 4.

Table 4. The finite element simulation conditions

parameter	value
polishing speed *v*（m/min）	31、40、50、56、62、70
polishing removal conditions（mm）	0.001、0.002、0.003、0.004

4. Results and discussion

4.1 Polishing process and surface morphology

Under the condition of polishing speed v=56m/min and polishing removal amount of 0.004mm, the finite element simulation polishing process is shown in Fig. 5.

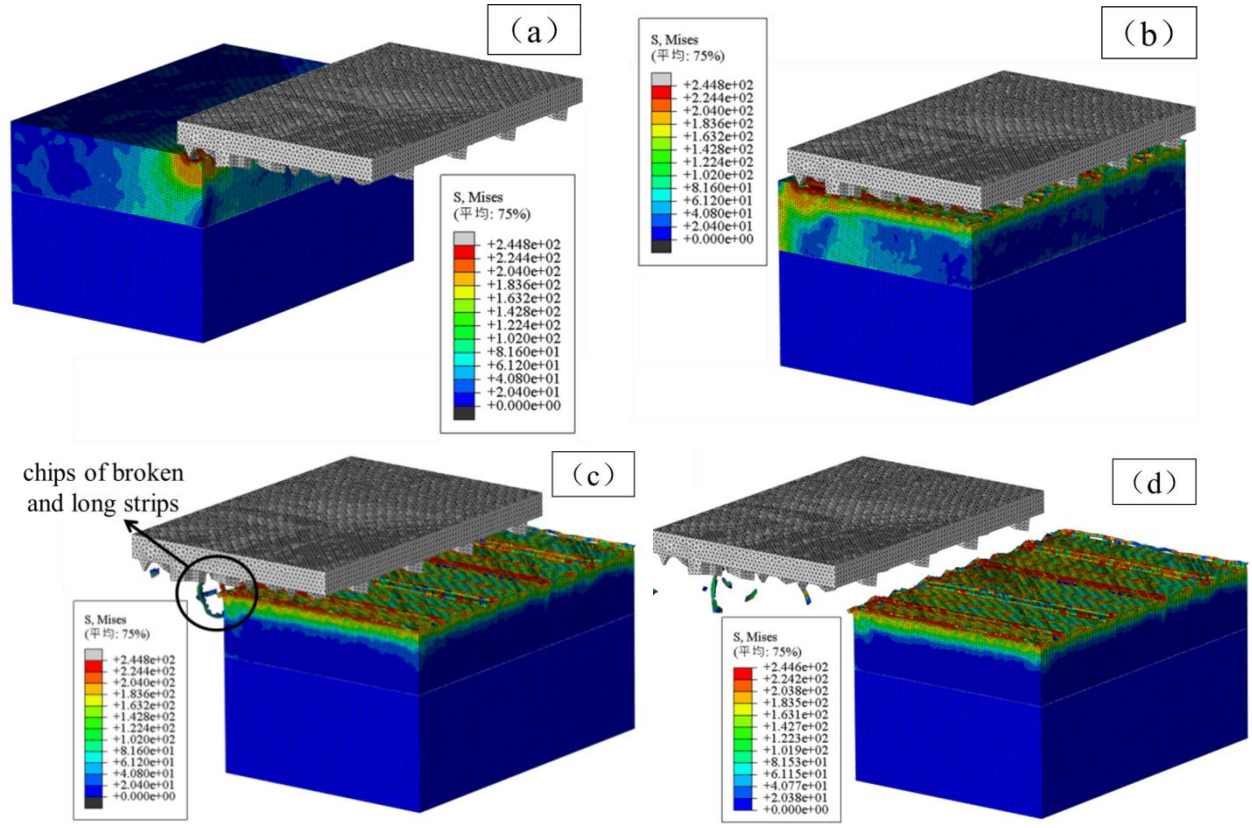

Fig. 5 The polishing process (polishing speed v=56m/min and polishing removal amount of 0.004mm)

As shown in Fig. 5(a), the sandpaper initially contacts with the hard anodic oxide film, and the maximum stress value of the hard anodic oxide film rapidly increases to about 244.8Mpa, and the stress is mainly distributed in the range of the hard anodic oxide film. As shown in Fig. 5(b), with the further feeding of sandpaper, the maximum stress is mainly distributed in the polishing surface area. Fig. 5(c) shows that the hard anodic oxide film has been basically removed by polishing, and the residual stress is mainly distributed in the surface layer within 0.0034 mm, and the chips produced by polishing are mainly broken and long strips with microscopic morphology. As shown in Fig. 5(d), after the sandpaper is separated from the hard anodic oxide film, the residual stress of the hard anodic oxide film is basically the same as that in Fig. 5(c), indicating that polishing mainly relies on the front part of the abrasive particles in the feeding direction of sandpaper, while the back part of the abrasive particles play a small role in polishing and mainly play a role in smoothing the polishing area.

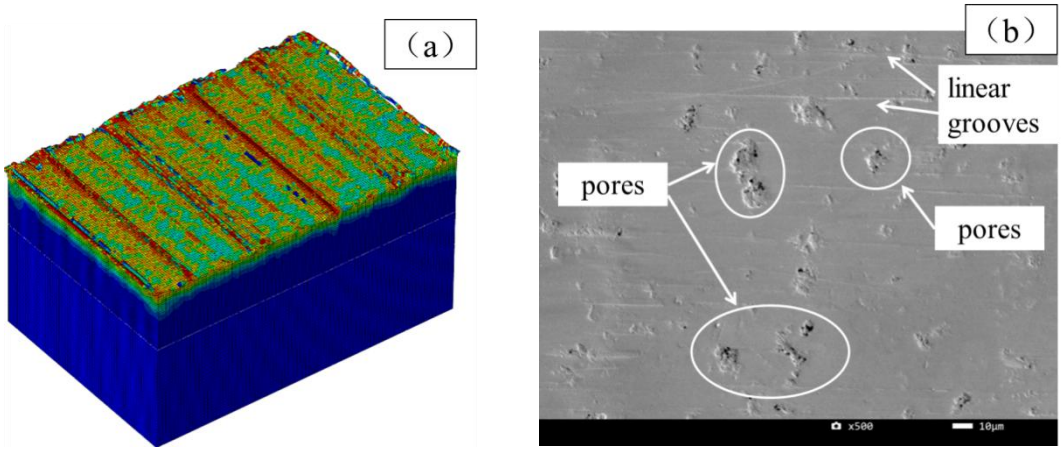

（a）Finite element analysis （b）SEM Photos

Fig. 6 The comparison of surface quality of hard anodic oxide film polishing

The comparison in Fig. 6 shows that under the action of sandpaper abrasive particles, certain grooves will be generated on the surface, and in the SEM photos, there are not only a certain number of grooves, but also more pits and pores, and the hard anodic oxide film is composed of barrier layer and porous layer, while the porous layer is composed of many hexaprismatic oxide units shaped like a honeycomb structure[12].

4.2 The finite-element results of polishing force

Under the conditions of polishing speed v=56m/min and polishing removal amount 0.004mm, the changes of normal polishing force *Fz* is shown in Fig. 7.

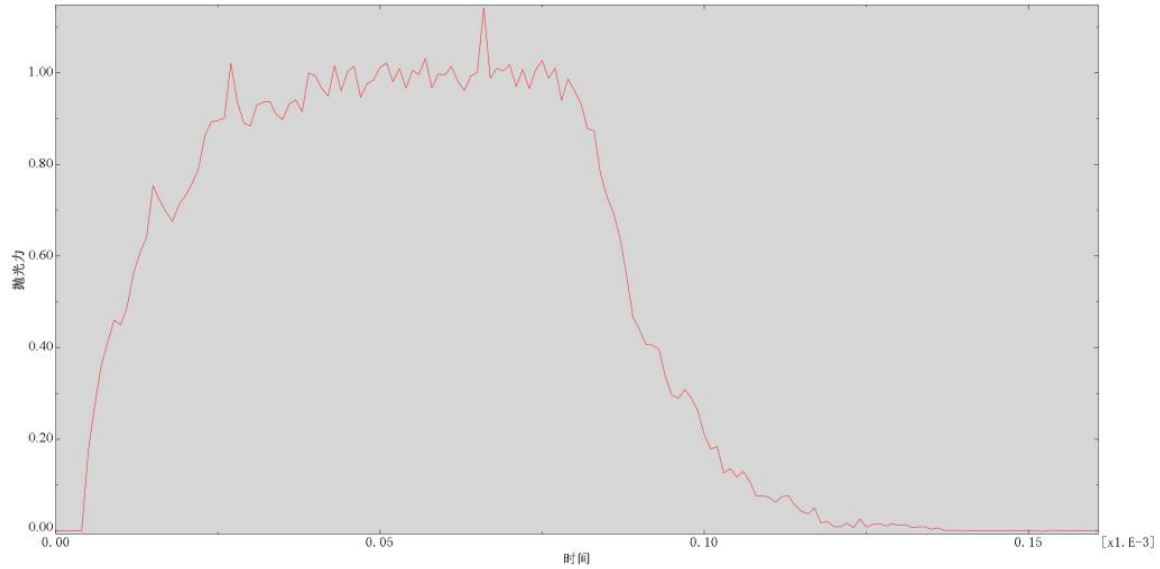

Fig. 7 The normal polishing force during polishing

As shown in Figure 7, after the initial contact between sandpaper and hard anodic oxide film, the polishing force starts to rise rapidly, and the polishing force reaches a peak average of 0.98N as the effective polishing area of the sandpaper is in full contact with hard anodic oxide film. The polishing force remains stable until the effective polishing area of the sandpaper begins to leave the hard anodic oxide film, and the polishing force decreases rapidly. Until the sandpaper all leaves the hard anodized film area, and the polishing force drops to 0.

4.3 The comparison of finite element simulation results and experimental results of polishing force

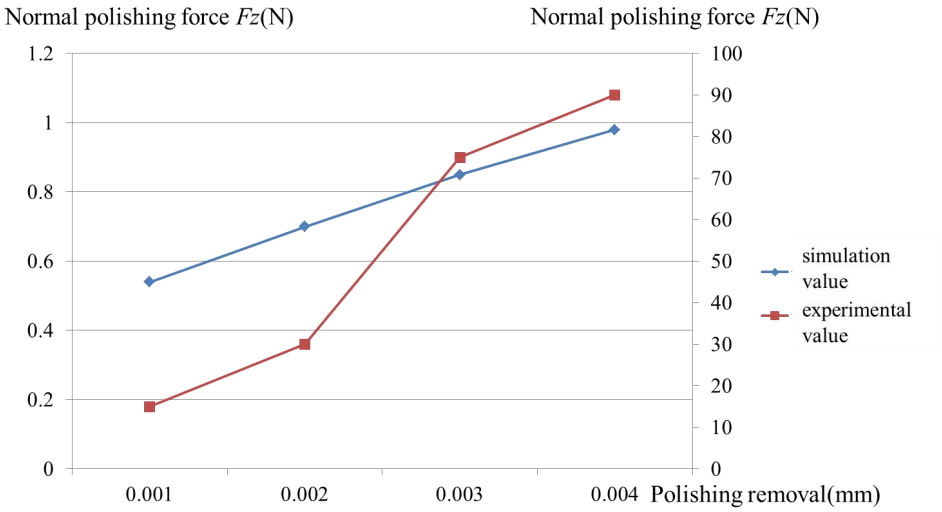

Fig. 8 The effect of polishing removal amount on normal polishing force

In the finite element simulation, different hard anodic oxide film removal amounts were used to calculate the polishing force under the condition of the same polishing speed as the test. As shown in Fig.8, the finite element polishing is at the microscopic level, and the calculated polishing force is consistent with the experimental polishing force in trend.

4.4 The result of finite element analysis of the effect of polishing parameters on polishing force

In order to study the effect of polishing speed and polishing removal amount on polishing force when polishing hard anodic oxide film with sandpaper, the finite element simulation test was carried out on hard anodic oxide film according to the finite element simulation conditions in Table 3. During the simulation process, only a single test condition was changed and the other polishing condition was remained constant, the effect of polishing speed on polishing force is shown in Fig. 9 and the effect of polishing removal amount on polishing force is shown in Fig. 10, and the polishing force is taken as the average value of the peak area shown in Fig. 7.

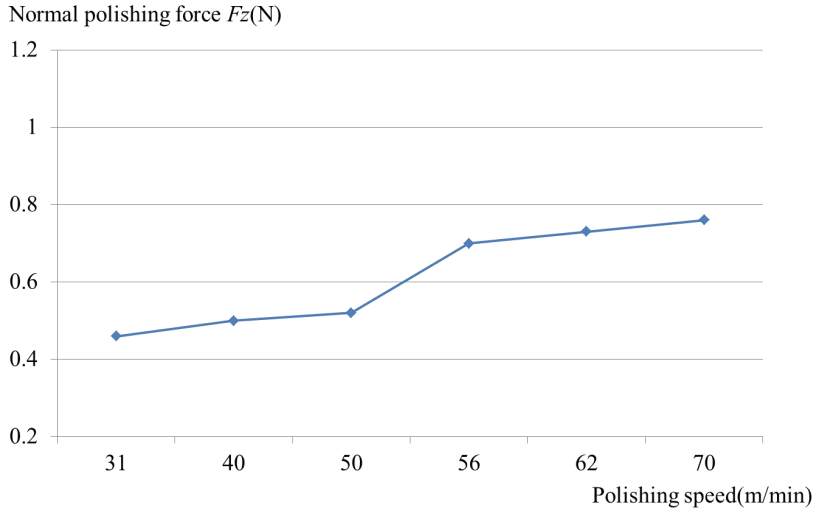

Fig. 9 The effect of polishing speed on polishing force

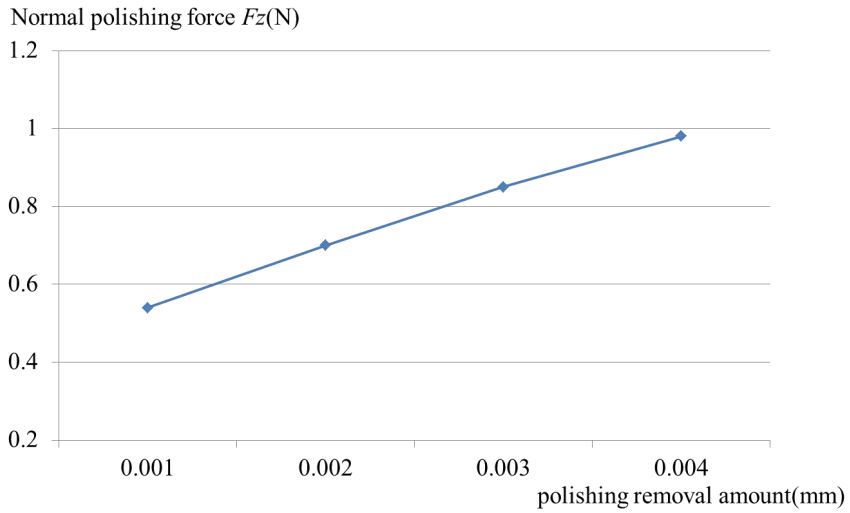

Fig. 10 The effect of removal amount on polishing force

As shown in Fig. 9, with the polishing speed increasing from 31m/min to 70m/min, the normal polishing force *Fz* increases from 0.46N to 0.76N in the process of polishing hard anodic oxide film, showing an overall upward trend. As shown in Fig. 10, the normal polishing force *Fz* increased from 0.54 to 0.98 N with the increase of polishing removal from 0.001 to 0.004 mm in the process of polishing hard anodic oxide film, showing an overall upward trend.

The comparison of Fig. 9 and Fig. 10 reveals that the polishing removal parameter has a greater degree of influence on the polishing force.

Conclusion

(1) In the polishing process, the residual stress on the surface after polishing is mainly distributed within 0.0034mm of the surface, and the chips produced by polishing are mainly broken and long strips with microscopic morphology, and polishing mainly depends on the abrasive particles in the front part of the sandpaper feed direction.

(2) Under the action of sandpaper abrasive particles, the results of finite element simulation and test show that there are certain grooves on the surface of oxide film, and in the SEM photos, there are not only a certain number of grooves, but also more pits and pores.

(3) The finite element simulation of the normal polishing force of hard anodic oxide film is consistent with the polishing test results.

(4) In the process of polishing hard anodic oxide film, the normal polishing force increases as the polishing speed increases; the normal polishing force increases as the polishing removal amount increases; the polishing removal amount parameter has a greater degree of influence on the polishing force.

Acknowledgment

This work was financially supported by Dalian High level Talent Innovation Support Plan (2021RQ042) fund.

References

[1] Liu Dabo, Yang Shoujie, Wang Kelu, Dong Xianjuan. Hot deformation behavior and processing diagram of 2D70 aluminum alloy. Chinese Journal of Nonferrous Metals, 2013, 23(08): 2077-2082.

[2] Wang Yanzhi. Advances in anodizing technology of aluminum and its alloys. Materials Protection, 2005, 34(9): 25-26.

[3] Wang Ping, Wei Xiaowei. Formation mechanism of multi-pass anodic oxide film. Surface Technology, 2005, 34(6): 28-32.

[4] Zhu Zufang. Anodizing and surface treatment of aluminum alloy. Beijing, Chemical Industry Press, 2004: 140-155.

[5] Wernick S., Pinner R., Sheasby P. G.. The surface treatment of aluminum and its alloys, 5th. England, Finishing Publications Ltd, 1987: 1023-1026.

[6] Zeng Xinlong, Wang Chunxia, Cai Xiaohan, et al. Effect of temperature on properties of 2A12 aluminum alloy hard anodized film. Plating and Finishing, 2018, 40(09): 6-9.

[7] Pan Wenbo, Lu Jiabin, Yan Qiusheng. Experimental study on cluster magnetorheological plane polishing of aluminum alloy anodized film. Lubrication and Sealing, 2018, 43(10): 45-50.

[8] Wielage B, Nickel D, Alisch G, et al. Effects of pre-treatment on the growth rate and morphology of hard anodic films onaluminium. Surface and Coatings Technology, 2007, 202(3): 569-576.

[9] Wan Hongqiang, Han Peiying, Ge Shuai, et al. Finite element analysis and experiment of ultrasonic composite abrasive vibration polishing method. Machine Tool and Hydraulics, 2020, 48(07): 38-42.

[10] Yang Jinming. Effect of anodizing treatment on diesel piston top on structural reliability. Shandong University of Technology, 2019.

[11] Zhu Jie, Zhu Liang, Chen Jianhong. Effect of stress triaxiality and strain rate on mechanical properties and material characterization of 6063 aluminum alloy. Journal of Materials Science and Engineering, 2007, 107(03): 358-362.

[12] Tang Hua. Study on hard anodizing technology and properties of 2A12 aluminum alloy. Nanchang Hangkong University, 2013.